ISSN 1063-7834, Physics of the Solid State, 2015, Vol. 57, No. 5, pp. 886–890. © Pleiades Publishing, Ltd., 2015.
Original Russian Text © S.S. Aplesnin, O.B. Romanova, A.M. Khar'kov, A.I. Galyas, 2015, published in Fizika Tverdogo Tela, 2015, Vol. 57, No. 5, pp. 872–876.

SEMICONDUCTORS

Investigation of the Transport Properties of Cation-Substituted Solid Solutions $Yb_xMn_{1-x}S$

S. S. Aplesnin[a, b], O. B. Romanova[a], A. M. Khar'kov[b], and A. I. Galyas[c]

[a] *Kirensky Institute of Physics, Siberian Branch of the Russian Academy of Sciences, Akademgorodok 50–38, Krasnoyarsk, 660036 Russia*

[b] *Reshetnev Siberian State Aerospace University, pr. imeni Gazety "Krasnoyarskii Rabochii" 31, Krasnoyarsk, 660014 Russia*

[c] *Scientific-Practical Materials Research Centre, National Academy of Sciences of Belarus, ul. P. Brovki 19, Minsk, 220072 Belarus*

e-mail: rob@iph.krasn.ru

Received September 24, 2014

Abstract—The electrical properties and thermopower of solid solutions $Yb_xMn_{1-x}S$ with substitution concentrations $0 < x \le 0.2$ have been studied in the temperature range of 77–1050 K. It has been found that the electrical conductivity has a semiconducting character, and the thermopower changes its sign from positive to negative as the substitution concentration in $Yb_xMn_{1-x}S$ increases. It has been established that the activation energy decreases with increasing ytterbium concentration. The model of impurity donor 4*f* states satisfactorily agrees with the data on the electrical resistivity and the thermopower.

DOI: 10.1134/S1063783415050029

1. INTRODUCTION

Compounds containing rare-earth elements exhibit unusual combination of the physical properties and are attractive in connection with the possibility of their use as the element base in microelectronics, spintronics, and sensor devices [1]. At the present time, magnetic materials demonstrating a strong correlation between the electrical and magnetic subsystems have been extensively studied; this correlation is observed in a number of phase transitions (such as metal-insulator and magnetic phase transitions, including changes in the magnetic properties without changes in the magnetic symmetry [2, 3]), as well as in the magnetoresistive effect. According to the earlier studies, promising materials for investigating these effects are cation-substituted compounds $Me_xMn_{1-x}S$ ($Me = 3d$ metal) [4, 5] and $Re_xMn_{1-x}S$ (Re = Gd, Sm) [5, 7] synthesized on the basis of the antiferromagnetic semiconductor manganese monosulfide. As a result of the studies of the electrical and thermoelectric properties of sulfides $Re_xMn_{1-x}S$ (Re = Gd, Sm), it was found that these compounds undergo metal-insulator phase transitions with variations in the Re concentration and temperature, the thermopower coefficient changes by several orders of magnitude as a function of the substituting element concentration, and the conductivity changes from the *p*-type to the *n*-type [8–10]. Gadolinium–manganese sulfide-based compounds have fairly high thermopower coefficients [11], which is of practical importance for designing new materials for temperature sensors widely used in metallurgy.

It is assumed that, when manganese cations are replaced with ytterbium ions, a pressure of the nearest environment leads to the change in the valence of ytterbium ions and to the formation of the metallic bond, as is the case in YbS compounds under pressure. At the normal pressure, ytterbium sulfide is a semiconductor with the direct gap of ~1.3 eV in the spectrum of electron excitations and the indirect gap of ~1.0 eV between the fully occupied 4*f* state and free *sd*-band states [12] lying 4 eV higher than the 3*p* valence band of sulfur ions. Under pressure, the gap decreases monotonically $dE_g/dp = -6 \pm 1$ eV/kbar [13]; at 8 GPa, the bands are overlapped and the metallic state is formed [14]. At 10 GPa, the quantum resonance, i.e., superposition of the f^{13} and f^{14} states and the change in the valence from 2 to 4, is observed. The charge carrier density per ytterbium ion is 0.4 [14].

If we take that the metal valence is +3 and the sulfur valence is –2, then, each of the unit cells containing four formula units YbS will contain four electrons which do not participate in the *Me*–S bond. These electrons will be transferred on the *Me*–*Me* bond and will be collectivized. The formation of the chemical bonds between ytterbium and manganese ions induces the transformation of the electronic structure in the solid solution and leads to a change in the transport properties.

The substitution of a rare-earth element for manganese shifts the *f* level. Here, there are several vari-

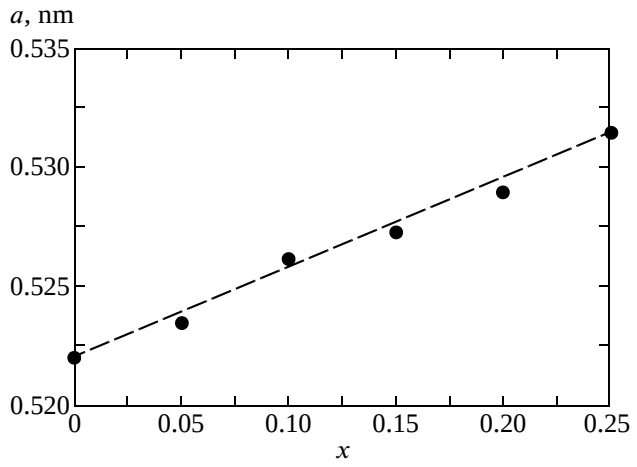

Fig. 1. Concentration dependence of the lattice parameter of $Yb_xMn_{1-x}S$ samples.

ants. If the *f* level is in the conduction band, an electron is transferred from the *Re* ion to the *d* level of the rare-earth ion or it remains below the conduction band bottom and continues to be bound to the donor. When the concentration of similar centers is low (i.e., less than the critical concentration at which the impurity band or the percolation threshold is formed), the material remains a semiconductor. In the case when the *f* level is in the band gap near the chemical potential, the temperature dependence of the resistance can exhibits extrema due to the shift of the chemical potential with increasing temperature. The proximity of the *f* level to the chemical potential can lead to significant magnitude of the thermopower.

As a result, a topical problem is to synthesize of new cation-substituted sulfide compounds $Yb_xMn_{1-x}S$ doped with rare-earth elements with variable valence and to determine the effect of the electronic structure and the radius of rare-earth Yb ion on the transport properties of $Yb_xMn_{1-x}S$ compounds over wide ranges of concentrations and temperatures.

2. EXPERIMENTAL RESULTS AND DISCUSSION

The synthesis of $Re_xMn_{1-x}S$ samples was described in [6, 15]. The X-ray diffraction study of the $Yb_xMn_{1-x}S$ sulfides was performed on a DRON-3 diffractometer in CuK_α radiation at a temperature of 300 K after their obtainment and after measurements. The X-ray diffraction shows that the synthesized compounds are single-phase and exhibit a face-centered cubic NaCl-type structure that is typical of manganese monosulfide. As the degree of cation substitution (*x*) increases, the unit cell parameter *a* increases linearly (Fig. 1).

The electrical resistance was measured by the compensation four-probe methods on direct current in the temperature range of 77–1050 K. The temperature

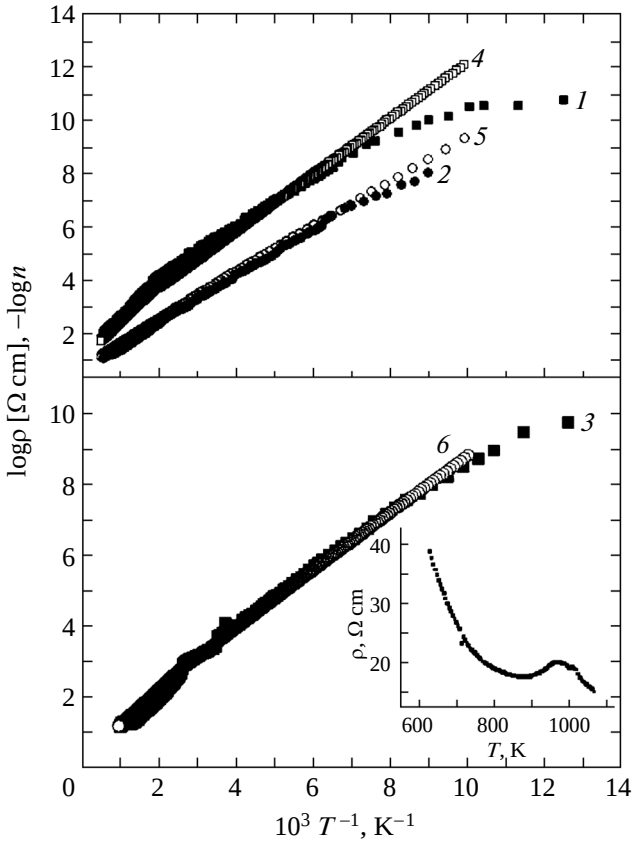

Fig. 2. Temperature dependences of the resistivity ρ of $Yb_xMn_{1-x}S$ sulfides with ytterbium concentrations $x =$ (*1*) 0.05, (*2*) 0.1, and (*3*) 0.15 and the electron concentration *n* in the conduction band according to the calculation from Eq. (1) with parameters (*4*) $E_g = 1.54$ eV, $E_{f0} = 0.51$ eV, and $A = 55$ eV K$^{-0.5}$ for $x = 0.05$; (*5*) $E_g = 1.37$ eV, $E_{f0} = 0.32$ eV, and $A = 8$ eV K$^{-0.5}$ for $x = 0.1$; and (*6*) $E_g = 1.2$ eV, $E_{f0} = 0.34$ eV, and $A = 25$ eV K$^{-0.5}$ for $x = 0.15$. The inset shows the temperature dependence of the resistivity for the composition with $x = 0.15$.

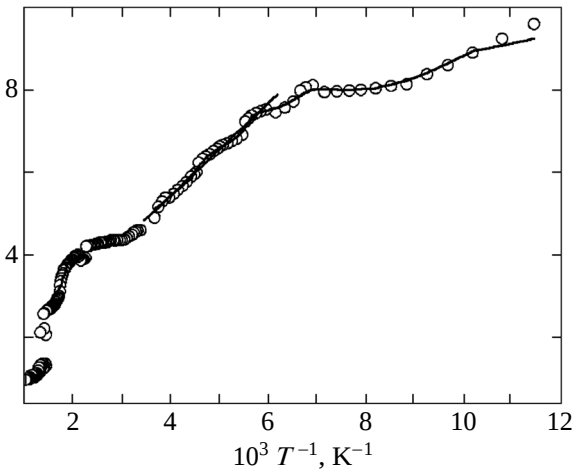

Fig. 3. Temperature dependence of the resistivity of $Yb_xMn_{1-x}S$.

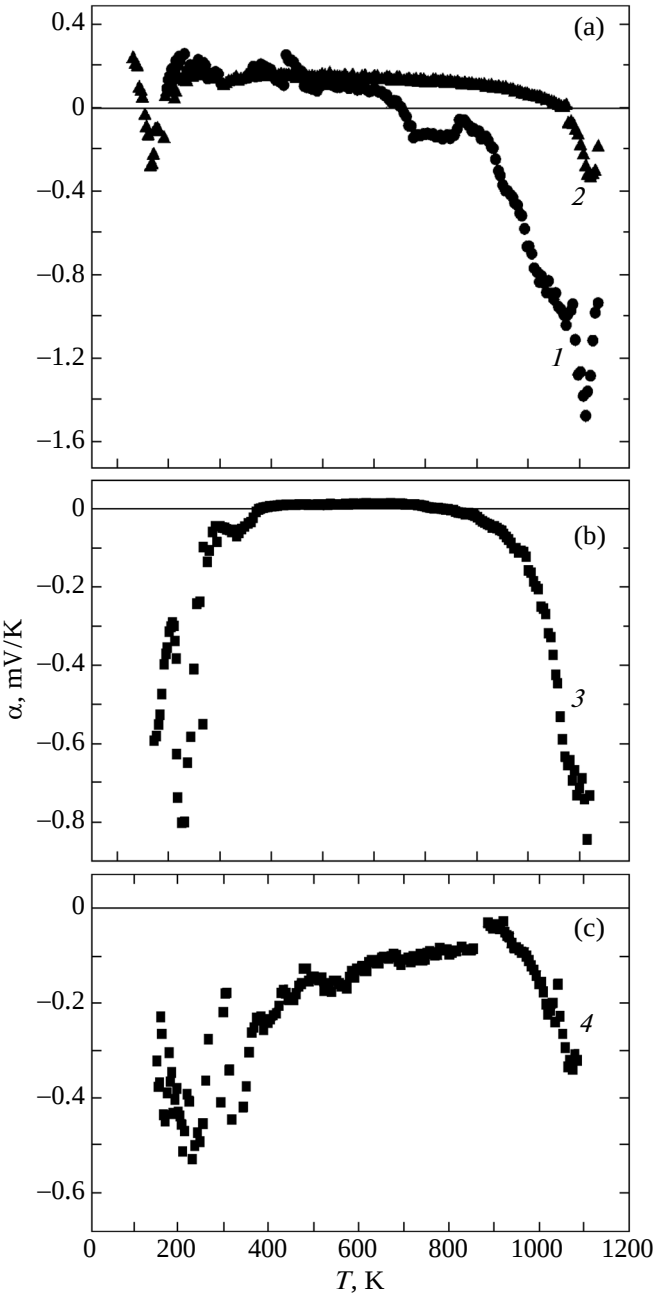

Fig. 4. Temperature dependences of the thermopower coefficient α of the compositions of solid solutions $Yb_xMn_{1-x}S$ with x = (*1*) 0.05, (*2*) 0.1, (*3*) 0.15, and (*4*) 0.2.

dependences of the resistivity of $Yb_xMn_{1-x}S$ solid solutions are shown in Figs. 2 and 3. They have typical semiconducting character in the compositions with $x \le 0.1$ and do not qualitatively differ on the temperature dependence of the resistivity of manganese monosulfide [16]. As the solid solution $Yb_{0.05}Mn_{0.95}S$ is heated, the activation energy increases by a factor of 1.7 at $T = 440$ K. As the substitution concentration x increases, the change in the value of the activation energy decreases, and the temperature shift to lower values to $T = 390$ K for $x = 0.1$. The substitution of ytterbium for manganese leads to the charge carrier concentration and the decrease in the activation energy. The energies of the impurity states E_i are below the conduction band bottom E_c in the energy gap. The absolute value of energy E_i decreases with increasing concentration.

The correlation between temperature dependences of the resistance and susceptibility can be found for the composition with $x = 0.15$ [17]. At $T = 288$ K, the electrical resistance exhibits a jump related to the decrease in the resistivity by a factor of two and the increase in the inverse susceptibility. At high temperatures 880 K $< T <$ 1020 K, the resistivity has a low maximum: $(\rho(T = 960\text{ K}) - \rho(T = 880\text{ K}))/\rho(T = 960\text{ K}) = 0.1$ (the inset in Fig. 2). This maximum is due to the coincidence of the 4*f* level and the Fermi level as it shifts from the conduction band bottom to the middle of the energy gap at high temperatures at which electrons are scattered on the *f* centers as a result of the *d*–*f* exchange.

In the composition with $x = 0.2$, the maximum disappears and the resistivity is changed stepwise by a factor of three at $T = 700$ K. This composition has two temperature ranges 110 K $< T <$ 150 K and 325 K $< T <$ 460 K, where the resistivity is independent of temperature, which is characteristic of the impurity-type semiconductors. In the vicinity of Néel temperature $T_N = 102$ K, the temperature derivative of the resistivity $d\rho(T)/dT$ has a maximum, which is typical for spin polarons. The formation of the jump of the resistivity at $T = 700$ K is likely due to the structural distortions in the lattice.

The substitution of ytterbium for manganese qualitatively changes the temperature dependence of the thermopower as compared to the case of MnS [16]. As temperature increases, the thermopower sign is changed from positive to negative at $T = 650$ K for $x = 0.05$ and also in the ranges 150 K $< T <$ 200 K and $T >$ 950 K for $x = 0.1$ (Fig. 4a). At the concentrations near the percolation concentration of ytterbium ions over the lattice, the thermopower is negative over entire temperature range and has two maximum (in magnitude) at $T = 225$ K and $T = 1000$ K for $x = 0.15$ (Fig. 4b) and $T = 245$ K and $T = 1090$ K for $x = 0.2$ (Fig. 4c). The low-temperature maxima are near the Debye temperature $T_D = 240$ K with the maximal density of the acoustic phonon modes and they are caused by the electron–phonon drag.

To explain the kinetic properties of $Yb_xMn_{1-x}S$ solid solutions, we consider the electronic structure of a semiconductor, where the donor level corresponding to 4*f* electrons of ytterbium is in the energy gap below

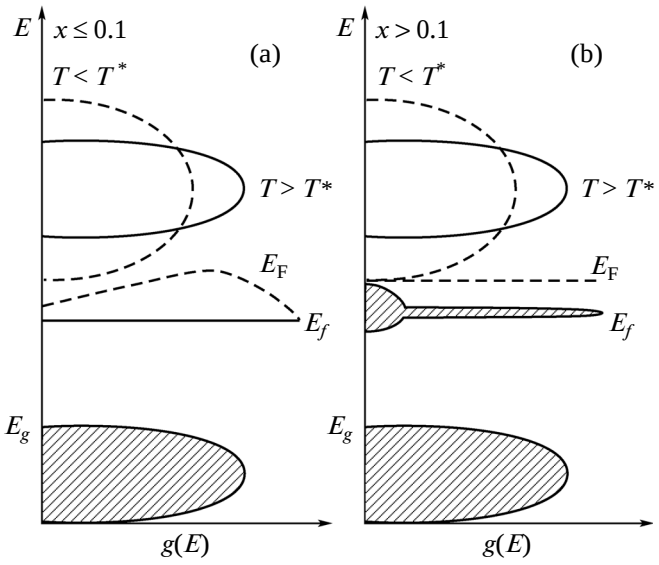

Fig. 5. Temperature dependences of the 4*f*-level energy E_f and the Fermi energy E_F determined from Eq. (1) with parameters (a) E_g = 1.54 eV, E_{f0} = 0.51 eV, and A = 55 eV K$^{-0.5}$ for x = 0.05 and (b) E_g = 1.2 eV, E_{f0} = 0.34 eV, and A = 25 eV K$^{-0.5}$ for x = 0.15.

the conduction band bottom. The equation for the Fermi energy has the form [18]

$$\begin{aligned} n_c\exp(-|E_F|/k_BT) &= n_i/[1+\exp((|E_F|-|E_f|)/k_BT)] \\ &+ \rho_v\exp((-|E_g|+|E_F|)/k_BT), \\ n_c &= 2((2\pi mnk_BT)/(2\pi h)^2)^{3/2}, \\ \rho_v &= 2((2\pi m_pk_BT)/(2\pi h)^2)^{3/2}. \end{aligned} \quad (1)$$

In the performed calculations, effective electron mass m_n is equal to hole mass m_p, and the energy in Eq. (1) is counted from the conduction band bottom (Fig. 5).

In what follows, we use the absolute values of the energies (E_F, E_f, E_g). The electron concentration at the 4*f* level corresponds to the ytterbium ion concentration $n_i = x$. In the temperature range 390 K < T < 440 K, the local modes of octahedra arranged near the Mn ion–Yb ion interface. The bending mode of the octahedron will lead to splitting the t_{2g} states of electrons, shifting the conduction band, and decreasing the energy interval between the *f* level and the conduction band bottom. This fact is taken into account in the model by a shift of the *f* level with respect to the conduction band bottom by a power law

$$\begin{cases} E_f = |A(T^* - T)^{0.5} + E_{f0}|, & T < T^* \\ E_f = |E_{f0}|, & T > T^*. \end{cases} \quad (2)$$

Three fitting parameters (A, the energy gap width E_g, and position of the 4*f* level E_{f0} with respect to the conduction band bottom) are determined from the conditions of the best coincidence of the temperature dependences of the conduction electron concentration with the experimental data on the resistivity, i.e., from the minimum of functional ($n(T) - \rho(T)$). At low and high temperatures, the activation energy is dependent on the position of impurity levels in the energy gap. Temperature T^*, at which the activation energy increases, was taken from the data on the resistivity. The temperature dependence of the calculated Fermi energy is shown in Fig. 5. At high temperatures, the Fermi energy and the 4*f* level are intersected for all compositions.

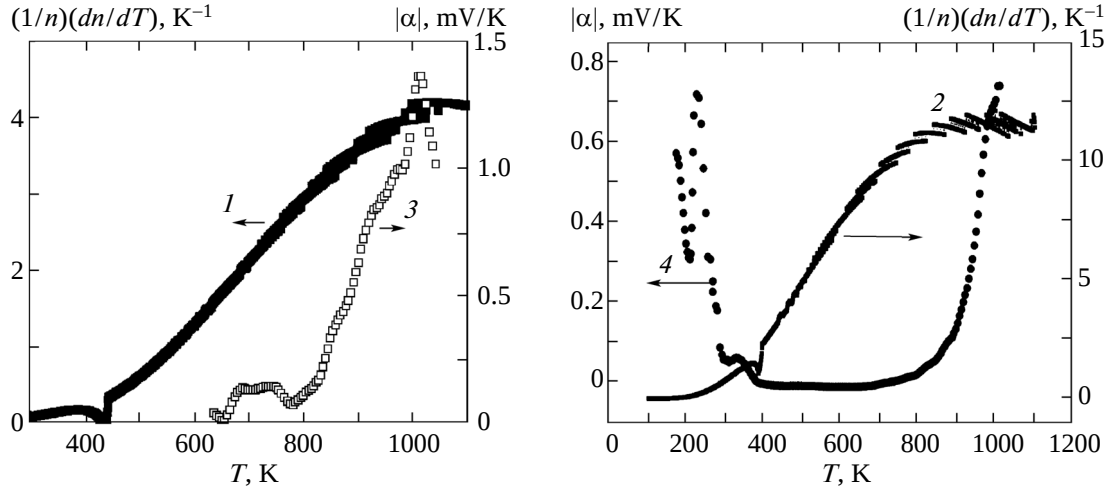

Fig. 6. Temperature dependences of the relative change in the electron concentration $(1/n)(dn/dT)$ calculated by Eq. (1) with parameters (*1*) E_g = 1.54 eV, E_{f0} = 0.51 eV, and A = 55 eV K$^{-0.5}$ for x = 0.05 and (*2*) E_g = 1.2 eV, E_{f0} = 0.34 eV, and A = 25 eV K$^{-0.5}$ for x = 0.15; and the temperature dependence of the thermopower absolute value for the $Yb_xMn_{1-x}S$ samples with x = (*3*) 0.05 and (*4*) 0.15.

Figure 2 shows the calculated temperature dependences of the charge carrier concentration for the following parameters: $E_g = 1.54$ eV, $E_{f0} = 0.51$ eV, and $A = 55$ eV K$^{-0.5}$ for $x = 0.05$; $E_g = 1.37$ eV, $E_{f0} = 0.32$ eV, and $A = 8$ eV K$^{-0.5}$ for $x = 0.1$; $E_g = 1.2$ eV, $E_{f0} = 0.34$ eV, and $A = 25$ eV K$^{-0.5}$ for $x = 0.15$. The satisfactory agreement between the charge carrier concentrations and the resistance in the dependence on temperature shows that the resistance mechanism is due to electrons of donor states of the $4f$ levels in the temperature range 100 K $< T <$ 800 K.

The high-temperature anomalies of the thermopower can be explained on the basis of the calculated temperature dependence of the charge carrier concentration. A temperature gradient leads to the formation of a diffusion electron current with current density $j = Dq|dn/dl| = Dq|dn/dT|(1/l)(dl/dT)l = Dql(|dn/dT|)(1/\beta)$, where D is the diffusion coefficient of electrons; q is the electron charge; l is the sample length, and β is the thermal expansion coefficient of the sample. We represent the potential difference in a closed circuit, in which there is a temperature gradient, as $U = El = j\rho l = l^2\rho qD(|dn/dT|)(1/\beta)$. In our samples, the electrical resistance is mainly determined by the charge carrier concentration $\rho \sim 1/n$, and the thermopower is $\alpha \sim (1/n)|dn/dT|$. The relative change in the concentration with variations in the temperature $(1/n)(dn/dT)$ is shown in Fig. 6; it has a maximum in the temperature range 950 K $< T <$ 1050 K, where the maximum magnitude of the thermopower is observed. At high temperatures, the theoretical estimates of the thermopower ~1 mV/K satisfactorily agree with the experimental data for $\rho = 0.1\ \Omega$ m, $\beta = 10^{-5}$ K^{-1}, and $D = 10^{-5}$ m^2/s.

3. CONCLUSIONS

Thus, we studied the effect of doping with the rare-earth element with variable valence (ytterbium) on the transport properties of $Yb_xMn_{1-x}S$ samples. As the manganese ions are replaced with ytterbium, the semiconducting type of the conductivity is conserved in the concentration range $0 < x < 0.2$. It was found that the activation energy increases upon heating of the samples of all compositions in the temperature range 380 K $< T <$ 440 K. It was revealed that the thermopower changes its sign, and also the charge carrier type also changes (from positive to negative) depending on the temperature at $x \le 1$ and the concentration. At concentrations near the concentration of percolation of ytterbium ions over the lattice, the thermopower has the maxima in magnitude at $T = 225$ and 1000 K for $x = 0.15$ and at $T = 245$ and 1090 K for $x = 0.2$. The high-temperature maximum is related to the electron diffusion and is due to the coincidence of the energies of the $4f$ level and the Fermi level; and the low-temperature maximum is due to the electron–phonon drag.

ACKNOWLEDGMENTS

This study was supported by the Russian Foundation for Basic Research (project nos. 12-02-00125_a and 15-02-01445_a).

REFERENCES

1. W. Ehrenstein, N. Mazur, and J. Scott, Nature (London) **442**, 759 (2006).
2. A. V. Golubkov, E. V. Goncharova, V. P. Zhuze, G. M. Loginov, V. M. Sergeeva, and I. A. Smirnov, *Physical Properties of Chalcogenides of Rare-Earth Elements* (Nauka, Leningrad, 1973) [in Russian].
3. S. S. Aplesnin, *Spin Liquid and Quantum Effects in Antiferromagnets* (Palmarium, Saarbrücken, Germany, 2012).
4. S. S. Aplesnin, O. B. Romanova, M. V. Gorev, D. A. Velikanov, A. G. Gamzatov, and A. M. Aliev, J. Phys.: Condens. Matter **25**, 025802 (2013).
5. S. S. Aplesnin, A. M. Har'kov, E. V. Eremin, O. B. Romanova, D. A. Balalev, V. V. Sokolov, and A. Yu. Pichugin, IEEE Trans. Magn. **47**, 4413 (2011).
6. L. I. Ryabinkina, O. B. Romanova, and S. S. Aplesnin, Bull. Russ. Acad. Sci.: Phys. **72** (8), 1050 (2008).
7. S. S. Aplesnin, L. I. Ryabinkina, O. B. Romanova, D. A. Velikanov, D. A. Balaev, A. D. Balaev, K. I. Yanushkevich, A. I. Galyas, O. F. Demidenko, and O. N. Bandurina, J. Exp. Theor. Phys. **106** (4), 765 (2008).
8. O. B. Romanova, L. I. Ryabinkina, V. V. Sokolov, A. Yu. Pichugin, D. A. Velikanov, D. A. Balaev, A. I. Galyas, O. F. Demidenko, G. I. Makovetskii, and K. I. Yanushkevich, Solid State Commun. **150**, 602 (2010).
9. S. Aplesnin, O. Romanova, A. Harkov, D. Balaev, M. Gorev, A. Vorotinov, V. Sokolov, and A. Pichugin, Phys. Status Solidi B **249**, 812 (2012).
10. S. S. Aplesnin and A. M. Khar'kov, Phys. Solid State **55** (1), 81 (2013).
11. A. I. Galyas, O. F. Demidenko, G. I. Makovetskii, K. I. Yanushkevich, L. I. Ryabinkina, and O. B. Romanova, Phys. Solid State **52** (4), 687 (2010).
12. K. Syassen, H. Winzen, H. G. Zimmer, H. Tups, and J. M. Leger, Phys. Rev. B: Condens. Matter **32**, 8246 (1985).
13. D. R. Adhikari, R. K. Upadhyay, V. K. Singh, and G. C. Joshi, Indian J. Theor. Phys. **50**, 119 (2002).
14. M. Matsunami, H. Okamura, A. Ochiai, and T. Nanba, Phys. Rev. Lett. **103**, 237202 (2009).
15. S. S. Aplesnin, L. I. Ryabinkina, O. B. Romanova, V. V. Sokolov, A. Yu. Pichugin, A. I. Galyas, O. F. Demidenko, G. I. Makovetskii, and K. I. Yanushkevich, Phys. Solid State **51** (4), 698 (2009).
16. H. H. Heikens, C. F. van Bruggen, and C. J. Haas, J. Phys. Chem. Solids **39**, 833 (1978).
17. S. S. Aplesnin, A. M. Kharkov, O. B. Romanova, M. N. Sitnikov, E. V. Eremin, M. V. Gorev, K. I. Yanushkvich, V. V. Sokolov, and A. Yu. Pichugin, J. Magn. Magn. Mater. **352**, 1 (2014).
18. N. A. Poklonskii, S. A. Vyrko, and S. L. Podenok, *Statistical Physics of Semiconductors* (KomKniga, Moscow, 2005) [in Russian].

Translated by Yu. Ryzhkov